

High-order soliton breakup and soliton self-frequency shifts in a microstructured optical fiber

M. G. Banaee and Jeff F. Young

*Department of Physics and Astronomy, Advanced Materials and Process Engineering Laboratory,
University of British Columbia, Vancouver, British Columbia, Canada V6T 1Z4*

Received August 5, 2005; revised February 6, 2006; accepted February 20, 2006; posted March 7, 2006 (Doc. ID 63837)

Ultrashort pulse propagation in a polarization-maintaining microstructured fiber (with 1 μm core diameter and 1.1 m length) is investigated experimentally and theoretically. For an 80 MHz train of 130 fs pulses with average powers up to 13.8 mW launched into the lowest transverse mode of the fiber, the output spectra consist of discrete, multiple solitons that shift continuously to lower energies. The number of solitons and the amount that they shift both increase with the launched power. All of the data are quantitatively consistent with solutions of the nonlinear Schrödinger equation, but only when the Raman nonlinearity is treated without approximation, and self-steepening is included. These results remove any ambiguity as to the nature of these multiple solitons; they arise owing to the breakup of high-order solitons in the presence of nonlinear processes beyond self-phase modulation. © 2006 Optical Society of America

OCIS codes: 190.5530, 060.5530.

1. INTRODUCTION

The incorporation of photonic crystals in optical fiber technology has opened up interesting and active research areas in optical communications and nonlinear optics.^{1–6} These microstructured fibers consist of a uniform core region (typically either air or silica) that is surrounded by a photonic crystal cladding layer that most commonly consists of a periodic, hexagonal array of air holes defined by silica walls. One of the most important properties of photonic crystal fibers (PCFs) is that, by engineering the cladding crystal parameters (air-hole size, pitch, and lattice type), one can create fibers with anomalous group-velocity dispersion (GVD) in the visible and near-infrared parts of the electromagnetic spectrum. The GVD of a fiber is important not only in optical communication systems but also in the context of the nonlinear propagation of light through fibers. When a fiber is operated in the anomalous dispersion regime, it is possible to excite optical solitons that propagate without distortion by canceling the effect of GVD through self-phase modulation.^{7,8}

PCFs offer a particularly attractive medium in which to study guided-wave nonlinear optics for two reasons. First, the index contrast between the silica core and the surrounding photonic crystal lattice is relatively large compared with conventional single-mode fibers, thus reducing the effective mode diameter.⁹ The smaller mode has a proportionally higher electric field strength in the silica-core region for a given guided power level. Second, by being able to tune the dispersion, it is possible to make fibers in which the anomalous dispersion region and the near-zero dispersion point are near 800 nm and therefore are accessible using convenient short-pulse laser systems.

Already, several groups have reported supercontinuum generation across the visible and near-infrared regions in short segments of PCFs pumped with laser pulses rang-

ing in duration from 20 fs to 0.8 ns, at average power levels of only a few milliwatts.^{10–14} The low-threshold powers make this system attractive for potential applications in dense wavelength-division multiplexing¹⁵ and optical metrology.¹⁶

The precise shape of the nonlinearly shifted output spectrum varies from fiber to fiber and is strongly dependent on the fiber dispersion as well as the wavelength, power, duration, and chirp of the input pulses. In some circumstances the output spectrum consists of one or more discrete peaks that can be either redshifted or both redshifted and blueshifted. Previous studies^{17,18} of ordinary silica fibers showed that a combination of four-wave mixing, stimulated Raman scattering, and self-phase modulation processes can result in either discrete or continuous spectral broadening, depending on the particular circumstances.

In the present work, discrete broadening of 130 fs pulses passing through 1.1 m of photonic crystal fiber with 1 μm core diameter and 1.6 μm pitch is investigated for a range of input powers as a function of the propagation distance. For certain excitation conditions, the output spectra contain several discrete spectral components that gradually redshift with increasing input power or length of propagation. The broadening is strictly to the red and is similar in some respects to the Raman self-frequency shifting reported by others¹⁹ in regular silica fiber and to spectra reported by others^{20,21} in PCFs. In previous studies^{20–23} that specifically address the appearance of multiple solitons in PCFs, a variety of explanations have been offered. Although recent work convincingly argues that multiple solitons can result from the breakup of a high-order soliton launched into the PCF, quantitative comparisons between the model and experimental results are limited.^{24,25} Below, we quantitatively compare model

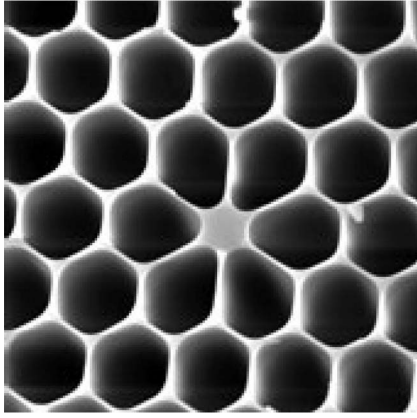


Fig. 1. A scanning electron micrograph, in cross section, of the photonic crystal fiber used in the experiment.

simulation results with a comprehensive set of measured spectra to convincingly demonstrate that the multi-soliton behavior observed in these experiments is due to the breakup of high-order solitons in the presence of Raman scattering and self-steepening. We also make clear that although the self-steepening term slightly modifies the rate at which the solitons Raman shift, the slowly varying envelope approximation applied to the Raman term leads to qualitatively different breakup characteristics that are inconsistent with the experimental results.

2. EXPERIMENT

Figure 1 shows a scanning electron micrograph of the cross section of a cobweb silica-based PCF (Crystal Fiber A/S, Denmark) used in this research. The PCF has $1\ \mu\text{m}$ core diameter and $\sim 1.6\ \mu\text{m}$ pitch. The objective of this study was to characterize the spectral properties of the light emanating from the PCF when subpicosecond pulses from a Ti:sapphire laser oscillating at a 80 MHz repetition rate are coupled into it using a $40\times$ microscope objective. By using a second-harmonic-generation-frequency-resolved-optical-gating setup, the duration of transform-limited pulses centered at 800 nm was measured to be 130 fs. The time-integrated output spectrum of the PCF was measured using a Fourier-transform spectrometer. The uniform spatial distribution and polarization of the fiber output confirmed that the coupled light propagates in a fundamental mode. The measured coupling efficiency was $\sim 11\%$.

3. RESULTS

Figure 2 shows the output spectra observed from a 1.1 m length of the fiber when it was pumped at 800 nm ($\sim 13.5\ \text{nm}$ bandwidth) for input average powers ranging from 10 to 120 mW (labels on the right of the figure show the measured output power for each case). At the highest powers used in the experiment ($\sim 14\ \text{mW}$ propagating in the fundamental mode), the output spectrum extended as far as 1000 nm and contained three well-separated spectral peaks. As Fig. 2 shows, the number of peaks in the output spectrum depends on the power, and the center wavelengths of these well-defined spectral components gradually redshift with increasing power. The square

symbols in Fig. 3 show the frequency shifts of the three well-separated spectral components in Fig. 2 versus power in the fundamental mode.

The development of the spectrum excited by a fixed input power was studied as a function of propagation distance in the fiber by bending the fiber at different lengths and by spectrally analyzing the radiation that leaked out of the core. Figure 4 shows the resulting spectra obtained at three points in the fiber when the average propagating power was 13.8 mW. As the figure shows, the center frequency of the well-separated peaks gradually decreases with increasing distance. The shifts of peaks in Fig. 4 are shown by the squares in Fig. 5.

Qualitatively similar experimental results have been reported before in both PCF^{22,23} and standard fiber,¹⁹ but often the Stokes components are accompanied by anti-Stokes components in the spectra, or the presence of multiple distinct spectral peaks is not obvious. Although the continuous shift to the red is clearly associated with Raman self-shifting solitons (RSSS),^{26,27} the origin of multiple peaks is less clear. At least one report²⁰ attributes multiple redshifted peaks to a set of RSSSs excited in different transverse spatial modes of the fiber. This cannot explain the results presented here, as there is no indication of high-order mode propagation in the spatial distribution of the output signal. Figure 6(a) and 6(b) show the

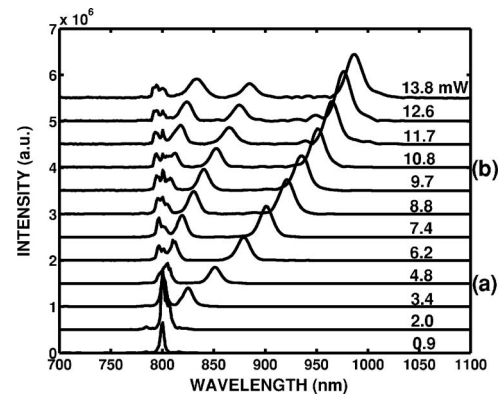


Fig. 2. Experimental output spectra of the photonic crystal fiber pumped at different average propagating powers (shown at right). The spectra marked with (a) and (b) have the most-shifted and the second-most-shifted solitons, respectively, centered at 850 nm.

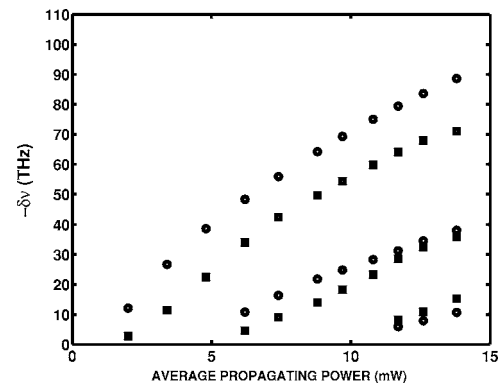


Fig. 3. Frequency shifts of the experimental peaks in Fig. 2 and simulated components from Fig. 7 versus average propagating power. Simulated results are marked with circles.

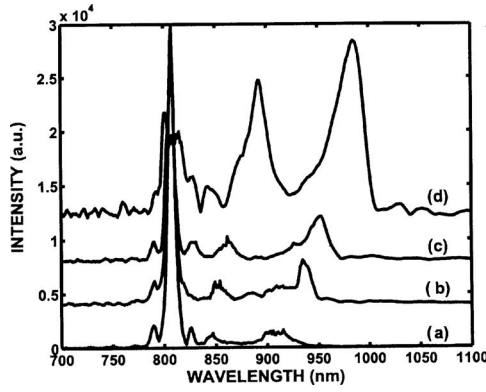


Fig. 4. Spectrum of the PCF bent at (a) 30, (b) 50, (c) 70 cm, and (d) the whole length of the fiber with 13.8 mW average power launched into the fundamental mode.

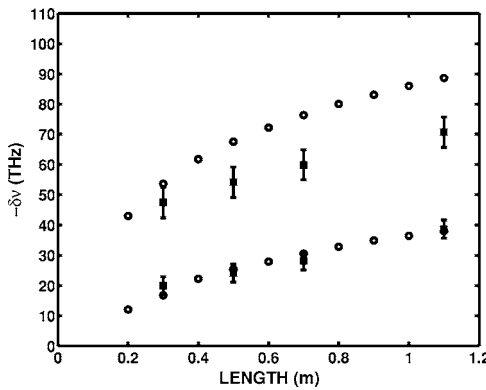


Fig. 5. Frequency shifts of the peaks in Fig. 4, and Fig. 8 versus propagation length. Squares represent the frequency shifts of the spectral components observed in the experiment and circles indicate the simulation values for shifts.

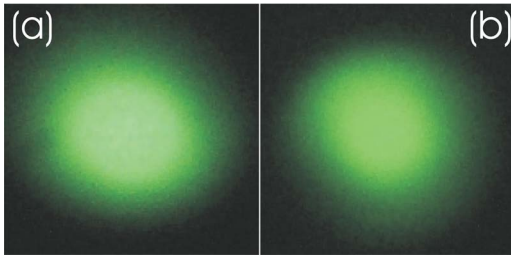


Fig. 6. (Color online) Spatial profile of the fiber output when (a) the most-shifted soliton is centered at 850 nm and (b) the second-most-shifted soliton is at 850 nm. These correspond to spectra (a) and (b), respectively, of Fig. 2.

far-field mode profile obtained by putting a bandpass filter centered at 850 nm at the fiber output when the first most-redshifted soliton, spectrum (a) in Fig. 2, and the second most-shifted soliton, spectrum (b) in Fig. 2, were centered at this wavelength.

Other reports^{21–24} assume that all observed solitons propagate in the same transverse mode of the fiber, and attribute them to a breakup of the high-order soliton launched into the fiber. This interpretation is supported by solutions of the nonlinear Schrödinger equation, augmented by additional nonlinear terms to take into account Raman scattering and self-steepening processes. In one case, semiquantitative agreement between the mea-

sured and the modeled spectral shifts of one of the fundamental RSSSs peaks as a function of incident power was reported.²⁴ The current experimental results, reported in Section 3, appear qualitatively consistent with the breakup of high-order solitons within a single transverse mode of the fiber. Below we show that simulations similar to those reported in Ref. 24 provide quantitative agreement with the measured power and propagation-distance dependences of all RSSS peaks. This removes any ambiguity about the origin of these multiple solitons, and it further shows that a full treatment of the Raman term (as opposed to the more commonly used, slowly varying envelope approximation^{28,29}), is essential to obtain this quantitative agreement between model and experiment.

4. DISCUSSION

A numerical model based on the split-step Fourier method²⁹ was used to solve the generalized nonlinear Schrödinger equation (GNLS), including high-order dispersion, Raman scattering, and self-steepening nonlinearities:

$$\frac{\partial A}{\partial z} = -\frac{\alpha}{2}A - \sum_{m=1}^6 \beta_m \frac{i^{m-1}}{m!} \frac{\partial^m A}{\partial t^m} + i\gamma \left(1 + \frac{i}{\omega_o} \frac{\partial}{\partial t} \right) \times \left[A(z, t) \int_{-\infty}^{+\infty} R(t') |A(z, t-t')|^2 dt' \right]. \quad (1)$$

In the above equation A is the envelope function, α is the linear loss, β_1 is the inverse of the group velocity, β_m (with $m \geq 2$) are higher-order dispersion coefficients, and γ is the nonlinear instantaneous Kerr effect coefficient. In Eq. (1) $R(t)$ is the response function of the guided medium:

$$R(t) = (1 - f_R)\delta(t) + f_R h_R(t), \quad (2)$$

which includes an instantaneous electronic contribution as well as vibrational Raman contributions, where $h_R(t)$ is the Raman response function of the silica core:

$$h_R(t) = \frac{\tau_1^2 + \tau_2^2}{\tau_1 \tau_2} \exp\left(-\frac{t}{\tau_2}\right) \sin\left(\frac{t}{\tau_1}\right), \quad (3)$$

with $\tau_1 = 12.2$ fs, $\tau_2 = 32.0$ fs, and $f_R = 0.18$.²⁹ The spectra obtained from the simulation for a fixed length of 1.1 m, for different propagating powers, are shown in Fig. 7, and the simulated spectra at different distances of propagation for a fixed propagating power of 13.8 mW are shown in Fig. 8.

In the above calculations we set $\gamma = 7.24 \times 10^{-8} (\mu\text{m}^2 \text{W})^{-1}$ (this value of γ is exactly what is expected if the light propagates in the fundamental spatial mode with the effective area set to the square of the pitch⁹). The dispersion coefficients used in the simulation results are fitted to the GVD curve in Fig. 9, which is calculated by the fiber manufacturer using a fully vectorial beam-propagation method.

The simulated results agree very favorably with those obtained experimentally. It is clear that Eq. (1) does describe how high-order solitons excited near the fiber input can spawn a series of fundamental Raman solitons that gradually shift to the red as they propagate. Figure 3

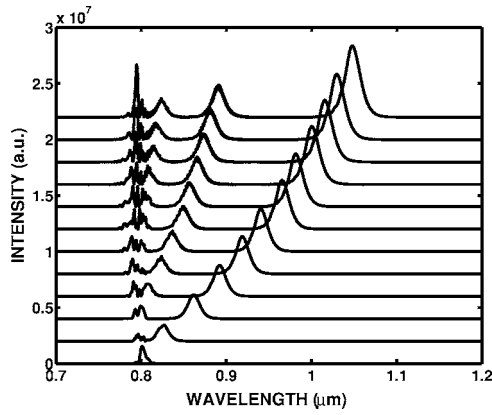


Fig. 7. Simulated spectra at different average propagating powers. Each spectrum was calculated for the same average propagating powers as in the experimental results shown in Fig. 2.

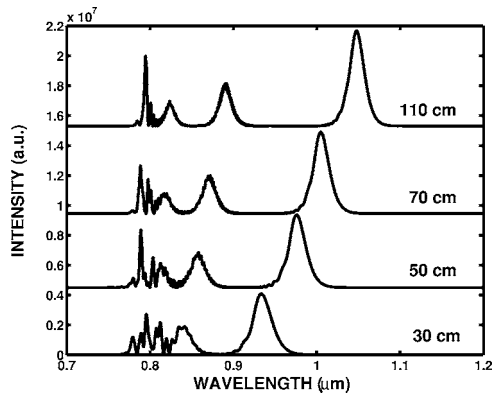


Fig. 8. Numerical solution of the GNLS equation. These are numerical spectra at four different lengths with 13.8 mW average propagating power.

compares the frequency shifts of spectral components in Figs. 2 and 7 versus power. Also, the shift of the center frequencies of the various discrete spectral components in Fig. 8 is plotted versus the length of propagation in Fig. 5, using circles.

To help interpret these results we use the well-known formula²⁹

$$N^2 = \frac{\gamma P_o T_o^2}{|\beta_2|} \quad (4)$$

to estimate the highest order of soliton that can be launched at the input of the fiber. With $\beta_2 = -1.625 \times 10^{-2} \text{ fs}^2/\mu\text{m}$ at 800 nm (dispersion curve in Fig. 9), the nonlinear coefficient $\gamma = 7.24 \times 10^{-8} (\mu\text{m W})^{-1}$, and the highest propagating peak power used in the experiment, one gets $N \approx 5$. A soliton of order 5 compresses to ~ 10.0 fs within the first few centimeters of its propagation through the fiber.³⁰ This occurs in the simulation results with or without the Raman and self-steepening terms in Eq. (1). When the Raman term is included, there is a sudden breakup of the compressing soliton just before it first reaches its minimum pulse duration, and three distinct RSSs gradually separate from the residual, complicated pulse that continues to propagate near the launch frequency. Each of the three RSSs has a distinct pulse du-

ration and peak power, which explains why they frequency shift at different rates. The self-steepening effect [term with the derivative in Eq. (1)] alone does not cause any soliton breakup in the output fiber spectrum but it slows the frequency shift of separate fundamental solitons.²⁵ Figure 10 compares the simulated spectra obtained with only the Raman term [Fig. 10(b)] and with both Raman and self-steepening [Fig. 10(a)] in the GNLS equation. It is worth mentioning that the high-order dispersion terms in Eq. (1), extracted from the GVD shown in Fig. 9, did not cause any soliton breakup when the Raman and self-steepening nonlinear terms in Eq. (1) were switched off.

It is difficult to quantitatively interpret the evolution of the pulses when the simulation is done with up to sixth-order dispersion. By including only second-order dispersion (a constant GVD across the entire spectrum), it is possible to verify that the various RSSs that are generated when high-order solitons break up after the initial compression are all fundamental solitons; their durations are inversely proportional to their amplitudes, with a

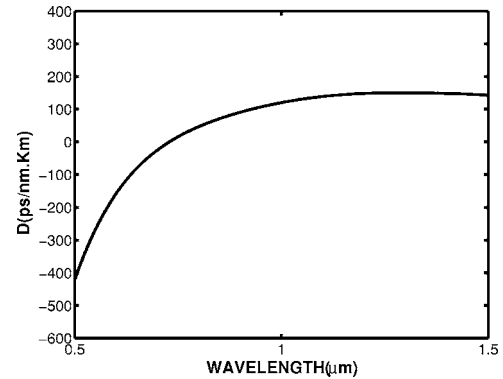


Fig. 9. Group-velocity dispersion used in the simulation. This is the dispersion calculated by using a fully vectorial beam-propagation method and an ideal approximation to the fiber cross section.

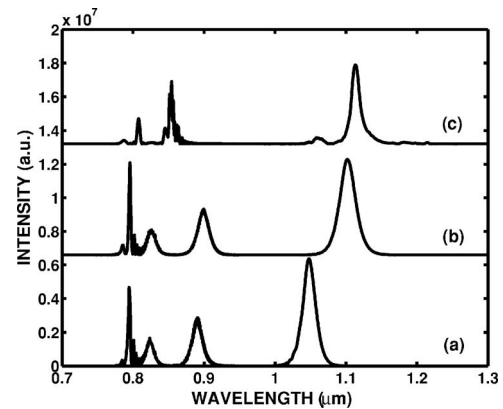


Fig. 10. Comparison of the simulated output spectra with 13.8 mW average propagating power, obtained from Eq. (1) (a) with all terms included, (b) neglecting the self-steepening term, and (c) by applying the slowly varying envelope approximation to the Raman term. Note that while the self-steepening term differentially modifies the rate of Raman shifting, the slowly varying envelope approximation fails to capture the proper soliton breakup.

fixed proportionality constant. This process of high-order soliton breakup in the presence of the Raman effect has been noted previously,^{31–33} but we believe that the current data and interpretation help to provide a better understanding of this interesting and potentially useful phenomenon.

For pulses with a duration longer than 100 fs, an approximate form of Eq. (1) is often used to simulate the pulse propagation in fibers.²⁹ The envelope function in the integration is simplified as

$$|A(z, t - t')|^2 \approx |A(z, t)|^2 - t' \frac{\partial}{\partial t} |A(z, t)|^2 \quad (5)$$

so that

$$\int R(t') |A(z, t - t')|^2 dt' \approx |A(z, t)|^2 - T_R \frac{\partial}{\partial t} |A(z, t)|^2, \quad (6)$$

where

$$T_R = \int t' R(t') dt' = f_R \int t' h_R(t') dt'. \quad (7)$$

By using the same Raman response function of silica as in the full simulation, Eq. (3), the T_R coefficient is 1.46 fs. Figure 10(c) shows the simulated spectrum with the approximated form of Eq. (1) and this value of T_R . This figure clearly shows that the approximate form of the Raman response cannot be used to describe the experimental results reported here.

5. CONCLUSION

The output spectrum of PCF, pumped by 130 fs pulses centered at 800 nm, exhibits discrete broadening of the incident pulse through creation of several fundamental solitons that continuously redshift with increasing power and propagation length. The far-field pattern of the fiber output as well as the similar spectral intensity for the most-shifted and second-most-shifted solitons at the same wavelength validate the idea of single spatial mode propagation of multiple solitons through this structure. The numerical solution of a generalized nonlinear Schrödinger equation that includes Raman scattering, self-steepening, and dispersion up to the sixth order provides a quantitative description of the experimental results, and it can be used to interpret the results as owing to the breakup of high-order solitons into fundamental self-shifting Raman solitons. The creation of these multiple fundamental Raman solitons suddenly happens when the launched pulse compresses to a critical pulse duration.

ACKNOWLEDGMENTS

We acknowledge the financial support of the Natural Sciences and Engineering Research Council of Canada, the Canadian Institute for Advanced Research, and the Canada Foundation for Innovation.

REFERENCES

1. J. C. Knight, T. A. Birks, P. St. J. Russel, and D. M. Atkin, "All-silica single-mode fiber with photonic crystal cladding," *Opt. Lett.* **21**, 1547–1549 (1996).
2. R. F. Cregan, B. J. Mangon, J. C. Knight, T. A. Birks, P. St. J. Russel, P. J. Roberts, and D. C. Allan, "Single-mode photonic bandgap guidance of light in air," *Science* **285**, 1537–1539 (1999).
3. K. Suzuki, H. Kubota, S. Kawanishi, M. Tanaka, and M. Fujita, "Optical properties of low-loss polarization-maintaining photonic crystal fiber," *Opt. Express* **9**, 676–680 (2001).
4. B. J. Eggleton, C. Kerbage, P. S. Westbrook, R. S. Windeler, and A. Hale, "Microstructured optical fiber devices," *Opt. Express* **9**, 698–713 (2001).
5. H. Lim, F. O. Ilday, and F. W. Wise, "Femtosecond ytterbium fiber laser with photonic crystal fiber for dispersion control," *Opt. Express* **10**, 1497–1502 (2002).
6. J. E. Sharping, M. Fiorentino, P. Kumar, and R. S. Windeler, "All-optical switching based on cross-phase modulation in microstructure fiber," *IEEE Photonics Technol. Lett.* **14**, 77–79 (2002).
7. I. F. Mollenhauer, R. H. Stolen, and J. P. Gordon, "Experimental observation of picosecond pulse narrowing and soliton in optical fiber," *Phys. Rev. Lett.* **45**, 1095–1098 (1980).
8. W. J. Wadsworth, J. C. Knight, A. Ortigosa-Blanch, J. Arriaga, E. Silvestre, and P. St. J. Russell, "Soliton effects in photonic crystal fibers at 850 nm," *Electron. Lett.* **36**, 53–55 (2000).
9. N. A. Mortensen, "Effective area of photonic crystal fibers," *Opt. Express* **10**, 341–348 (2002).
10. S. Coen, A. H. L. Chau, R. Leonhardt, J. D. Harvey, J. C. Knight, W. J. Wadsworth, and P. St. J. Russell, "Supercontinuum generation by stimulated Raman scattering and parametric four-wave mixing in photonic crystal fiber," *J. Opt. Soc. Am. B* **19**, 753–764 (2002).
11. J. M. Dudley, L. Provino, N. Grossard, H. Maillotte, R. S. Windeler, B. J. Eggleton, and S. Coen, "Supercontinuum generation in air-silica microstructured fibers with nanosecond and femtosecond pulse pumping," *J. Opt. Soc. Am. B* **19**, 765–771 (2002).
12. S. Coen, A. H. L. Chau, R. Leonhardt, J. D. Harvey, J. C. Knight, W. J. Wadsworth, and P. St. J. Russell, "White-light supercontinuum generation with 60-ps pump pulses in a photonic crystal fiber," *Opt. Lett.* **26**, 1356–1358 (2001).
13. A. Apolonski, B. Povazay, A. Unterhuber, W. Drexler, W. J. Wadsworth, J. C. Knight, and P. St. J. Russell, "Spectral shaping of supercontinuum in a cobweb photonic-crystal fiber with sub-20-fs pulses," *J. Opt. Soc. Am. B* **19**, 2165–2170 (2002).
14. W. J. Wadsworth, A. Ortigosa-Blanch, J. C. Knight, T. A. Birks, T. P. M. Man, and P. St. J. Russell, "Supercontinuum generation in photonic crystal fibers and optical fiber tapers: a novel light source," *J. Opt. Soc. Am. B* **19**, 2148–2155 (2002).
15. H. Takara, T. Ohara, K. Mori, K. Sato, E. Yamada, Y. Inoue, T. Shibata, M. Abe, T. Morioka, and K.-I. Sato, "More than 1000 channel optical frequency chain generation from single supercontinuum source with 12.5 GHz channel spacing," *Electron. Lett.* **36**, 2089–2090 (2000).
16. R. Holzwarth, Th. Udem, T. W. Hansch, J. C. Knight, W. J. Wadsworth, and P. St. J. Russell, "Optical frequency synthesizer for precision spectroscopy," *Phys. Rev. Lett.* **85**, 2264–2267 (2000).
17. P. L. Baldeck and R. R. Alfano, "Intensity effects on the stimulated four photon spectra generated by picosecond pulses in optical fibers," *J. Lightwave Technol.* **5**, 1712–1715 (1987).
18. R. H. Stolen, "Phase-matched-stimulated four-photon mixing in Silica-fiber waveguides," *IEEE J. Quantum Electron.* **11**, 100–103 (1975).
19. P. Beaud, W. Hodel, B. Zysset, H. P. Weber, "Ultrashort pulse propagation, pulse break up, and fundamental

- soliton formation in a single-mode optical Fiber," *IEEE J. Quantum Electron.* **23**, 1938–1946 (1987).
20. D. T. Reid, I. G. Cormack, W. J. Wadsworth, J. C. Knight, and P. St. J. Russell, "Soliton self-frequency shift effects in photonic crystal fiber," *J. Mod. Opt.* **49**, 757–767 (2002).
21. B. R. Washburn, S. E. Ralph, P. A. Lacourt, J. M. Dudley, W. T. Rhodes, R. S. Windeler, and S. Coen, "Tunable near-infrared femtosecond soliton generation in photonic crystal fibers," *Electron. Lett.* **37**, 1510–1512 (2001).
22. B. R. Washburn, S. E. Ralph, and R. S. Windeler, "Ultrashort pulse propagation in air-silica microstructure fiber," *Opt. Express* **10**, 575–580 (2002).
23. A. Ortigosa-Blanch, J. C. Knight, and P. St. J. Russell, "Pulse breaking and supercontinuum generation with 200-fs pump pulses in photonic crystal fibers," *J. Opt. Soc. Am. B* **19**, 2567–2572 (2002).
24. G. Genty, M. Lehtonen, H. Ludvigsen, J. Broeng, and M. Kaivola, "Spectral broadening of femtosecond pulses into continuum radiation in microstructured fibers," *Opt. Express* **10**, 1083–1098 (2002).
25. C. F. Chen and S. Chi, "Femtosecond second-order solitons in optical fiber transmission," *Optik* **116**, 331–336 (2005).
26. F. M. Mitschke and L. F. Mollenauer, "Discovery of the soliton self-frequency shift," *Opt. Lett.* **11**, 659–661 (1986).
27. J. P. Gordon, "Theory of the soliton self-frequency shift," *Opt. Lett.* **11**, 662–664 (1986).
28. G. Dong and Z. Liu, "Soliton resulting from the combined effect of higher-order dispersion, self-steepening and nonlinearity in an optical fiber," *Opt. Commun.* **128**, 8–14 (1996).
29. G. P. Agrawal, *Nonlinear Fiber Optics* (Academic, 2001).
30. L. F. Mollenauer, R. H. Stolen, J. P. Gordon, and W. J. Tomlinson, "Extreme picosecond pulse narrowing by means of soliton effect in single-mode optical fibers," *Opt. Lett.* **8**, 289–291 (1983).
31. A. Hasegawa and M. Matsumoto, *Optical Solitons in Fibers* (Springer, 2003).
32. W. Hodel and H. P. Weber, "Decay of femtosecond higher-order solitons in an optical fiber induced by Raman self-pumping," *Opt. Lett.* **12**, 924–926 (1987).
33. K. Tai, A. Hasegawa, and N. Bekki, "Fission of optical solitons induced by stimulated Raman effect," *Opt. Lett.* **13**, 392–394 (1988).